

Allosteric Interactions Required for High-Affinity Binding of Dihydropyridine Antagonists to $\text{Ca}_v1.1$ Channels Are Modulated by Calcium in the Pore

Blaise Z. Peterson and William A. Catterall

Department of Cellular and Molecular Physiology, The Penn State Milton S. Hershey College of Medicine, Hershey, Pennsylvania (B.Z.P.); and Department of Pharmacology, University of Washington, Seattle, Washington (W.A.C.)

Received November 11, 2005; accepted May 4, 2006

ABSTRACT

Dihydropyridines (DHPs) are an important class of drugs, used extensively in the treatment of angina pectoris, hypertension, and arrhythmia. The molecular mechanism by which DHPs modulate Ca^{2+} channel function is not known in detail. We have found that DHP binding is allosterically coupled to Ca^{2+} binding to the selectivity filter of the skeletal muscle Ca^{2+} channel $\text{Ca}_v1.1$, which initiates excitation-contraction coupling and conducts L-type Ca^{2+} currents. Increasing Ca^{2+} concentrations from approximately 10 nM to 1 mM causes the DHP receptor site to shift from a low-affinity state to a high-affinity state with an EC_{50} for Ca^{2+} of 300 nM. Substituting each of the four negatively charged glutamate residues that form the ion selectivity filter with neutral glutamine or positively charged lysine residues results in mutant channels whose DHP binding

affinities are decreased up to 10-fold and are up to 150-fold less sensitive to Ca^{2+} than wild-type channels. Analysis of mutations of amino acid residues adjacent to the selectivity filter led to identification of Phe-1013 and Tyr-1021, whose mutation causes substantial changes in DHP binding. Thermodynamic mutant cycle analysis of these mutants demonstrates that Phe-1013 and Tyr-1021 are energetically coupled when a single Ca^{2+} ion is bound to the channel pore. We propose that DHP binding stabilizes a nonconducting state containing a single Ca^{2+} ion in the pore through which Phe-1013 and Tyr-1021 are energetically coupled. The selectivity filter in this energetically coupled high-affinity state is blocked by bound Ca^{2+} , which is responsible for the high-affinity inhibition of Ca^{2+} channels by DHP antagonists.

Ca^{2+} entry through voltage-gated Ca^{2+} channels initiates a variety of cellular processes, including neurotransmitter release, muscle contraction, and gene expression. Voltage-gated Ca^{2+} channels are heteromultimeric complexes consisting of α_1 , β , γ , and α_2/δ subunits. The α_1 subunit is the pore-forming subunit and contains the key structural determinants required for gating, drug binding, and ion permeation (Fig. 1A). Ca^{2+} channels of the Ca_v1 subfamily conduct L-type Ca^{2+} currents and are the target proteins for a number of drugs, including the dihydropyridines (DHPs). DHPs are allosteric modulators of channel gating and may act as either agonists favoring an *open* state (Brown et al., 1984; Hess et al., 1984; Kokubun and Reuter, 1984; Thomas et al., 1985; Sanguinetti et al., 1986) or antagonists favoring *closed* states of the channel (Bean, 1984; Sanguinetti and Kass,

1984; Gurney et al., 1985; Kokubun et al., 1986; Cohen and McCarthy, 1987; Hamilton et al., 1987). Although it is clear that DHPs modulate channel-gating mechanisms, the molecular basis for DHP action remains unknown.

Localizing the DHP receptor site was an important first step toward elucidating the mechanism by which DHPs modulate Ca^{2+} channel gating. Nine key residues important for drug binding and unique to DHP-sensitive channels were localized to transmembrane segments IIIS5, IIIS6, and IVS6 (Mitterdorfer et al., 1996; Peterson et al., 1996; Schuster et al., 1996; He et al., 1997; Peterson et al., 1997). When these nine L-type-specific amino acids are substituted into a DHP-insensitive α_1 subunit, the resulting channel becomes sensitive to both DHP agonists and antagonists (Hockerman et al., 1997; Ito et al., 1997; Sinnegger et al., 1997). These studies indicate that transmembrane segments IIIS5, IIIS6, and IVS6 (Fig. 1A, dark cylinders) form the DHP receptor site.

The Ca^{2+} channel pore contains a Ca^{2+} binding site consisting of one negatively charged glutamate residue from each domain, which collectively form the selectivity filter

This work was supported by American Heart Association grant 0230298N (to B.Z.P.) and National Institutes of Health grants R01-HL074143 (to B.Z.P.) and P01-HL44948 (to W.A.C.).

Article, publication date, and citation information can be found at <http://molpharm.aspetjournals.org>.
doi:10.1124/mol.105.020644.

ABBREVIATIONS: DHP, dihydropyridine; PN200-110, 4-(4-benzofurazanyl)-1,4-dihydro-2,6-dimethyl-3,5-pyridinedicarboxylic acid methyl 1-methyl ester.

(Fig. 1). The selectivity filter is thought to consist of a negatively charged locus capable of binding a single Ca^{2+} with high affinity or two Ca^{2+} ions with low affinity (Hille, 2001; Sather and McCleskey, 2003). In the absence of divalent cations, Ca^{2+} channels are highly permeable to monovalent cations. Under such conditions, Ca^{2+} functions as a channel blocker with an IC_{50} in the submicromolar range. Monovalent currents are blocked by Ca^{2+} ions because monovalent cations are unable to dislodge tightly bound Ca^{2+} ions from the selectivity filter. Currents carried by Ca^{2+} ions occur when Ca^{2+} is raised to the millimolar range because repulsive forces from a second Ca^{2+} ion entering the pore increase the exit rate of the bound Ca^{2+} ion by more than 10,000-fold at physiological Ca^{2+} concentrations (Almers and McCleskey, 1984; Hess and Tsien, 1984; Yue and Marban, 1990). The original two-site barrier model nicely simulates most of the permeation properties of the channel, but it has limited value when applied to structural studies. However, the primary features of this model (i.e., binding and repulsion) almost certainly are dominant forces in a conducting pore.

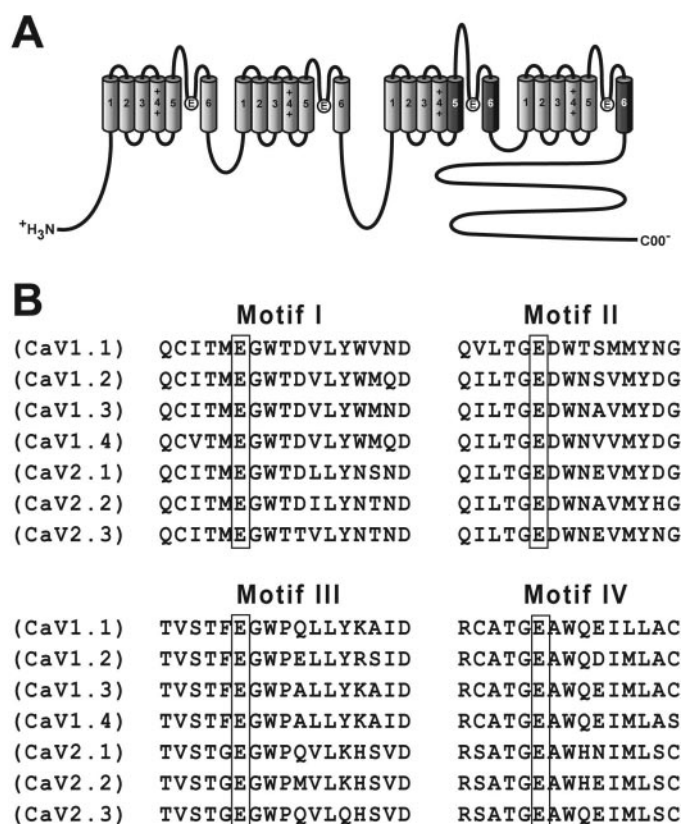


Fig. 1. The selectivity filter consists of four negatively charged glutamate residues that bind a single Ca^{2+} ion with a high affinity or two Ca^{2+} ions with a low affinity. **A**, the α_{1S} subunit of the Ca^{2+} channel consists of four homologous repeats (I, II, III, and IV) that assemble to form the pore of the channel complex. Each repeat consists of six transmembrane segments, S1–S6. The loops connecting the 5th and 6th transmembrane segments from each repeat contain highly conserved glutamate residues (denoted with an E) that collectively form the selectivity filter. The selectivity filter is capable of binding a single Ca^{2+} ion with a high affinity or two Ca^{2+} ions with a low affinity. Dihydropyridine agonists and antagonists interact with amino acid residues located in transmembrane segments IIIS5, IIIS6, and IVS6 (dark cylinders). **B**, the pore segments from each of the four domains of the DHP-sensitive ($\text{Ca}_v1.1-4$) and -insensitive ($\text{Ca}_v2.1-3$) Ca^{2+} channels are aligned. The Ca^{2+} binding glutamate residues that form the selectivity filter are indicated with boxes.

Binding and repulsion of ions within the selectivity filter are core features of recent models of the pore that are based more on structure than the original two-site models (Dang and McCleskey, 1998; Nonner et al., 1998; Boda et al., 2001; Corry et al., 2001; Lipkind and Fozzard, 2001).

We and others have found that high-affinity DHP binding is dependent on Ca^{2+} binding to the selectivity filter (Mitterdorfer et al., 1995; Peterson and Catterall, 1995). These findings establish an important link between DHP binding to its receptor site deep within the lipid bilayer and Ca^{2+} binding to the selectivity filter in the outer pore. This relationship offers a unique opportunity to gain a deeper understanding of the molecular basis for DHP action, ion permeation, and gating. We have systematically characterized the DHP and Ca^{2+} binding characteristics of mutant Ca^{2+} channels whose pore-forming glutamate residues have been replaced by glutamine or lysine. We analyzed these mutants using an allosteric binding model that enabled us to determine 1) the actual dissociation constants for Ca^{2+} binding to the selectivity filter at any DHP concentration, 2) the dissociation constant for DHP binding at any Ca^{2+} concentration, and 3) the magnitude of two allosteric factors that couple DHP and Ca^{2+} binding. We found that all four of the glutamate residues that form the ion selectivity filter are important for DHP and Ca^{2+} binding. Mutational analysis of several non-glutamate residues in the outer pore revealed altered DHP and Ca^{2+} sensitivity as well. Thermodynamic mutant cycle analysis (Carter et al., 1984; Hidalgo and MacKinnon, 1995) of two of these mutants, F1013G and Y1021K, indicate that Phe-1013 and Tyr-1021 are energetically coupled when a single Ca^{2+} ion is bound in the selectivity filter, suggesting that DHP binding promotes structural rearrangements in the outer pore that involve the energetic coupling of Phe-1013 and Tyr-1021 via a single bound Ca^{2+} ion. We discuss our findings in the context of current theoretical and structural models for permeation (Nonner et al., 1998; Boda et al., 2001; Corry et al., 2001; Lipkind and Fozzard, 2001; Wang et al., 2005) and propose that DHPs block monovalent and divalent currents by stabilizing a nonconducting blocked state that is structurally and functionally analogous to a channel with a single Ca^{2+} ion in its selectivity filter.

Materials and Methods

Preparation of Wild-Type and Mutant $\text{Ca}_v1.1$ Membranes. Wild-type and mutant α_{1S} ($\text{Ca}_v1.1$) Ca^{2+} channels were coexpressed with the β_{1a} and $\alpha_{2\delta}$ subunits as described previously (Peterson and Catterall, 1995). In brief, cDNAs encoding all the channel subunits were cotransfected into tsA-201 cells by calcium phosphate precipitation, and membranes were harvested 2 to 3 days after transfection. Cells were washed twice in buffer A (50 mM Tris, 100 μM phenylmethylsulfonyl fluoride, 100 μM benzamidinium 1.0 μM pepstatin A, 1.0 $\mu\text{g}/\mu\text{l}$ leupeptin, and 2.0 $\mu\text{g}/\text{ml}$ aprotinin, pH 8.0). Cells were scraped and homogenized in the same buffer using a glass-Teflon homogenizer. The homogenate was centrifuged at 1700g for 10 min, and the resulting pellet was discarded. The supernatant was centrifuged at 100,000g for 30 min, and the resulting membrane pellet was washed and homogenized in buffer A. Membrane aliquots remained stable for several months, but they were typically used within 1 week of harvesting.

Radioligand Binding. Saturation binding assays were performed in buffer A using 20 to 100 μg of membrane protein, 0.1 to 10 nM (+)-[^3H]PN200-110 (PerkinElmer Life and Analytical Sciences, Boston, MA), and the indicated concentrations of free Ca^{2+} for 120

min at 22°C. Nonspecific binding was determined by the addition of 1 μM (\pm)-PN200-110, thus reducing k_{on} for the radiolabeled ligand to an insignificant level, and bound radioligand was recovered by vacuum filtration using GF/C glass fiber filters.

Experiments that measure the Ca^{2+} dependence of [^3H](+)-PN200-110 binding were performed on membranes prepared from cells expressing wild-type and mutant Ca^{2+} channels. Membranes were incubated in buffer A containing [^3H](+)-PN200-110 at a concentration producing an occupancy of 0.5 in optimal Ca^{2+} [i.e., equal to the dissociation constant for [^3H](+)-PN200-110 for that channel determined by saturation binding in 1 mM free Ca^{2+}], and the indicated concentrations of free Ca^{2+} . Free Ca^{2+} was buffered by the addition of 5 mM EDTA, 5 mM *N*-2[2-hydroxyethyl]-EDTA, and 5 mM nitrilotriacetic acid, and the amounts of CaCl_2 required to yield the desired concentrations of free Ca^{2+} were determined using the Ca^{2+} -buffering calculator MAXC (Chris Patton, Stanford University, Stanford, CA).

Data Analysis. DHP binding as a function of Ca^{2+} concentration was fit using an allosteric binding model (Fig. 2B, Scheme 1) described in the text with the aid of the analysis and graphics programs Excel (Microsoft, Redmond, WA) and Origin (OriginLab Corp., Northampton, MA). The statistical significance of the observed differences between the binding parameters of wild-type and mutant

channels was evaluated using a two-tailed Student's *t* test and analysis of variance (Fig. 3). Data are means \pm S.E.M., and statistical significance was set at $P < 0.05$ (*).

Results

An Allosteric Binding Model Describes the Positive Cooperativity between DHP and Ca^{2+} Binding. The DHP receptor site can exist in multiple affinity states depending on the level of Ca^{2+} present (Glossmann et al., 1985; Mitterdorfer et al., 1995; Peterson and Catterall, 1995). In Fig. 2A, membranes derived from cells expressing the wild-type skeletal muscle Ca^{2+} channel ($\text{Ca}_v1.1$) were tested for binding using the DHP antagonist [^3H](+)-PN200-110 in the presence of the indicated concentrations of free Ca^{2+} . Increasing the free Ca^{2+} from less than 10 nM to 100 μM causes a substantial increase in the level of (+)-PN200-110 binding with an EC_{50} of approximately 0.33 μM , followed by a reduction in binding with an IC_{50} of more than 100 mM. We initially fit these data using an allosteric model where a single DHP receptor site could exist in one of three interconvertible affinity states dependent on whether zero, one, or two divalent cations bound to the channel (Peterson and Catterall, 1995). We later found that this model could not adequately describe our data under all experimental conditions. For example, the EC_{50} values measured in our Ca^{2+} response experiments are dependent on the concentration of DHP used in the experiment—i.e., increasing DHP levels shift the EC_{50} to the left and decreasing DHP levels shift the EC_{50} to the right. Therefore, we revised this model such that it is now thermodynamically constrained and better describes the allosteric behavior of our system (Fig. 2B, Scheme 1). This revised version of Scheme 1 is superior to its predecessor for three main reasons: 1) the true dissociation constants for Ca^{2+} binding to the selectivity filter at any DHP concentration can now be determined; 2) two of the three independent dissociation constants for DHP binding have been eliminated; and 3) two coupling factors, α and β , have been introduced that couple DHP and Ca^{2+} binding. Using this revised version of Scheme 1 (Fig. 2B), we are now able to quantitatively assess the binding affinity for Ca^{2+} to the channel and the cooperativity between the Ca^{2+} and DHP receptor sites. It turns out that α , which was absent in the original model, is altered in several of the most interesting mutant channels assessed in these studies (see below).

Figure 2B, Scheme 1, is thermodynamically constrained such that the ratio of dissociation constants for DHP binding in the absence and presence of Ca^{2+} must equal to the ratio of the dissociation constants for Ca^{2+} binding in the absence and presence of DHP. Therefore, the individual dissociation constants for DHP and Ca^{2+} binding are completely determined by K_{D1} , the dissociation constant for DHP binding to a channel whose selectivity filter is occupied by a single Ca^{2+} ion, and K_{C1} , the dissociation constant for Ca^{2+} binding to DHP-occupied Ca^{2+} channels, respectively, and the allosteric factors α and β .

Ca^{2+} Binding to the Outer Pore Is Allosterically Coupled to DHP Binding. The pore segments from each domain of DHP-sensitive ($\text{Ca}_v1.1$ -4) and -insensitive ($\text{Ca}_v2.1$ -3) Ca^{2+} channels are aligned in Fig. 1B. To determine whether Ca^{2+} binding to the pore is allosterically coupled to DHP binding, each of the negatively charged glutamate residues

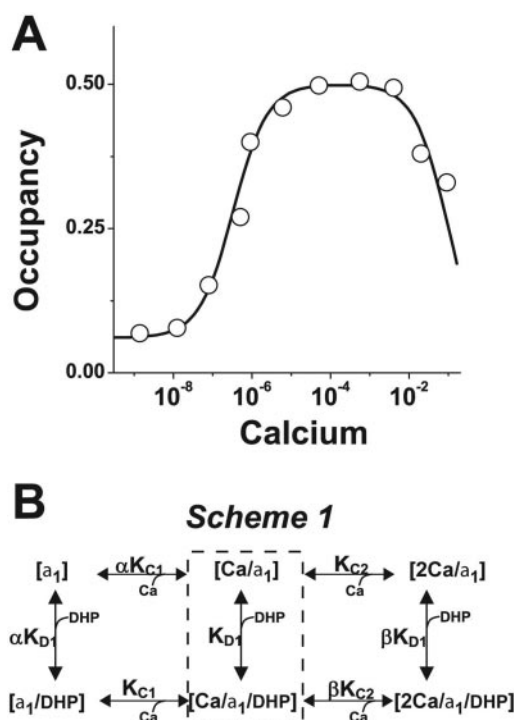


Fig. 2. Ca^{2+} is a positive allosteric modulator of DHP binding. A, membranes prepared from cells expressing wild-type Ca^{2+} channels were incubated with [^3H]PN200-110 at a concentration equal to its dissociation constant measured in 1 mM free Ca^{2+} ($1 \times K_{\text{D1}}$) and the indicated concentrations of free Ca^{2+} (see *Materials and Methods*). Data from one such experiment (circles) demonstrate that increasing Ca^{2+} from 10 nM to 1 mM results in a large increase in DHP binding with an EC_{50} of approximately 0.3 μM . Further increases in Ca^{2+} to the 100 mM range result in a large decrease in DHP binding with an IC_{50} in the high millimolar range. The line is a smooth fit through the data points and was generated using Scheme 1 (B). Scheme 1 describes $\text{Ca}_v1.2$ as possessing a single DHP receptor site that can exist in one of three affinity states, depending on whether zero, one, or two Ca^{2+} ions are bound to the selectivity filter. Scheme 1 is thermodynamically constrained such that dissociation constants for DHP and Ca^{2+} binding are coupled by the factors α and β . High-affinity DHP binding stabilizes a nonconducting, blocked state that is structurally analogous to a channel with a single Ca^{2+} ion in its selectivity filter (dashed box). Scheme 1 is further described in the text.

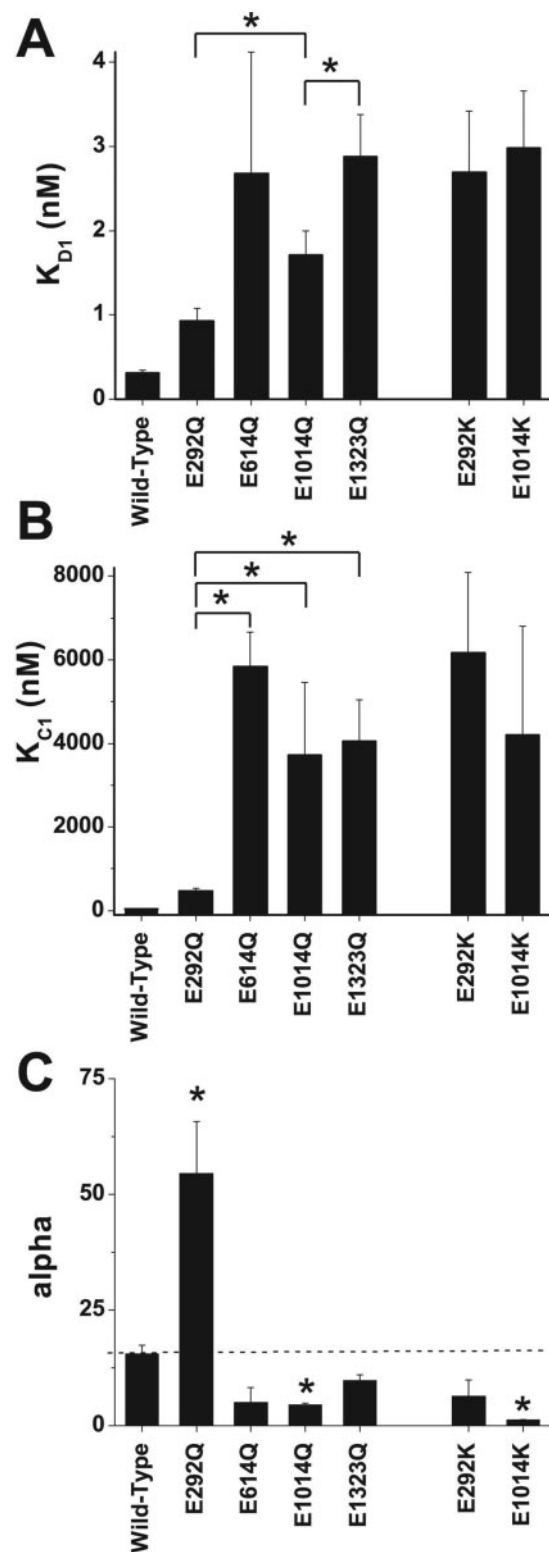


Fig. 3. Ca^{2+} binding to the selectivity filter is allosterically coupled to DHP binding. A and B, individual dissociation constants, K_{D1} (A) and K_{C1} (B), were determined for [^3H]PN200-110 and Ca^{2+} binding to wild-type and the indicated mutant channels as described under *Materials and Methods*. K_{D1} and K_{C1} values for all glutamine and lysine substitutions are significantly different from wild type. K_{C1} for the glutamine substitutions are significantly different from wild type. K_{D1} values for E292Q and E1014Q are significantly different from E1323Q but not E614Q. C, values for the coupling factor α were determined as described under *Materials and Methods* using Fig. 2B, Scheme 1 (also see Fig. 2A).

that collectively form the selectivity filter (Fig. 1B, boxes) was replaced by a neutral glutamine or a positively charged lysine residue, generating the mutants E292Q, E614Q, E1014Q, E1323Q, E292K, E614K, E1014K, and E1323K. E614K and E1323K exhibited no DHP binding and were not studied further. K_{D1} for each mutant was determined by saturation binding in the presence of 1 mM free Ca^{2+} and increasing concentrations of (+)-PN200-110. K_{D1} values for wild-type and each of the mutant channels are summarized in Fig. 3A and Table 1. The sensitivity of the wild-type and mutant channels to Ca^{2+} was determined by incubating membranes in a concentration of (+)-PN200-110 equal to the measured K_{D1} value for that particular channel (resulting in an occupancy of 0.5) plus increasing concentrations of free Ca^{2+} , as described under *Materials and Methods*. K_{C1} and α were determined by fitting these data using Fig. 2B, Scheme 1, with K_{D1} and free (+)-PN200-110 serving as fixed parameters. K_{D1} , K_{C1} , and α for wild-type and each mutant channel are summarized in Fig. 3 and Table 1.

DHP binding, the sensitivity of DHP binding to Ca^{2+} , and the coupling factor α are altered for the mutant channels. The values determined for K_{D1} are increased 5.5- to 10-fold by these mutations (Fig. 3A; Table 1). Although the four glutamate residues are not contiguously localized on the primary sequence, each functions as an important DHP binding determinant in the presence of Ca^{2+} , suggesting that the selectivity filter acts as a unified locus that modulates DHP binding. Alteration of the four glutamate residues affects K_{D1} , K_{C1} , and α to different extents. These differences indicate that the binding site for Ca^{2+} ions is asymmetrical, as is the coupling of each glutamate residue to DHP binding (Fig. 3).

As expected for mutant channels with amino acid substitutions in their selectivity filters, dramatic changes in K_{C1} were observed (Fig. 3B). The smallest change in K_{C1} was observed with E292Q, whose binding of Ca^{2+} is reduced by less than 12-fold. K_{C1} for the other glutamate mutants was increased by 90- to 150-fold.

The allosteric coupling factor α , which reflects the effect of binding of one Ca^{2+} ion on DHP affinity, was reduced from 15.5 for wild type to values ranging from 1.3 to 9.8 for the glutamate substitution mutants (Fig. 3C). E292Q, whose value for α was increased to 54.5, was the only exception to this trend. The role α plays in determining DHP binding properties is discussed in greater detail below. Together, the changes in K_{D1} , K_{C1} , and α in these mutants indicate that the DHP receptor site is allosterically coupled to the selectivity filter of L-type Ca^{2+} channels. Therefore, it is plausible that the molecular details that underlie DHP activity may involve structural rearrangements in the outer pore and selectivity filter of the channel.

Uncharged Residues in the Outer Pore Are Critical for DHP and Ca^{2+} Binding. A comparison of the amino acid sequences in the outer pore segments of each repeat of the Ca^{2+} channel isoforms reveals several residues that are unique to DHP-sensitive channels and are adjacent to the Ca^{2+} binding glutamate residues in the selectivity filter (Fig. 1B). To determine whether these residues are important DHP- and/or Ca^{2+} binding determinants, the mutants C288A, F1013G, Q1018E, Q1018M, Y1021K, C1319A, Q1326H, and E1327Q were constructed and analyzed as described above and under *Materials and Methods* (Fig. 4;

Table 2). C288A, Q1018E, Q1018M, C1319A, Q1326H, and E1327Q have DHP and Ca^{2+} binding profiles similar to those of wild type and are not discussed further.

In contrast to the glutamate mutants, high-affinity binding of DHP and Ca^{2+} is enhanced for mutant F1013G, in which a glycine conserved in all Ca_v2 channels is substituted for a phenylalanine residue that is present in all $\text{Ca}_v1.1$ channels. K_{D1} for F1013G is slightly lower than that of wild type (0.22 versus 0.31 nM, respectively), and K_{C1} for F1013G decreased 2.3-fold from 40 to 17.4 nM (Fig. 4, A and B). However, the most interesting change in the binding profile for F1014G is the 12.5-fold increase in magnitude of the coupling factor α which results in an 11-fold increase in αK_{D1} compared with wild type (Fig. 4C).

High-affinity binding of DHP and Ca^{2+} is also modified for mutant Y1021K, in which a lysine residue found in $\text{Ca}_v2.1$ and $\text{Ca}_v2.2$ channels is substituted for a tyrosine residue found in all $\text{Ca}_v1.1$ channels (Fig. 4). First, in contrast to F1013G, K_{D1} for Y1021K is 3-fold larger than K_{D1} for wild type (Fig. 4A; Table 2). Second, K_{C1} for Y1021K is more than 30-fold larger than K_{C1} for wild type (Fig. 4B). Finally, although the coupling factor α for F1013G is 12.5-fold larger than that of wild type, α for Y1021K is only one-half that of wild type (Fig. 4C).

The results with F1013G and Y1021K indicate that non-glutamate residues in the outer pore loop function as important binding determinants for DHPs and Ca^{2+} ions. The qualitative differences in the effects of these mutations on ligand binding suggest that the roles Phe-1013 and Tyr-1021 play in DHP and Ca^{2+} binding are distinct.

Ca^{2+} Promotes Energetic Coupling between Phe-1013 and Tyr-1021. Qualitatively divergent effects of Ca^{2+} on DHP binding affinity were observed with the mutants F1013G and Y1021K (Fig. 4; Table 2), even though these two substitutions typically coexist in Ca_v2 channels within the same nine-amino acid segment of the outer pore loop of domain III (Fig. 1B). This prompted us to construct a mutant channel in which Phe-1013 and Tyr-1021 have been replaced with glycine and lysine, respectively, resulting in the double mutant FY/GK. The double mutation causes a much larger increase in K_{D1} than either single mutation (Fig. 4A; Table 2), whereas the values of K_{C1} and α are intermediate between the two single mutants (Fig. 4, B and C; Table 2). Thus, the parameters for DHP and Ca^{2+} binding to FY/GK differ substantially from the sum of those for the single mutants, indicating that the two residues interact energetically in their function as DHP and Ca^{2+} binding determinants.

Thermodynamic mutant cycle analysis (Carter et al., 1984; Hidalgo and MacKinnon, 1995) was used to quantitate the energetic interaction between Phe-1013 and Tyr-1021 in DHP binding (Fig. 5). The coupling energy ($RT\ln\Omega$) between Phe-1013 and Tyr-1021 was calculated in nominally zero Ca^{2+} using αK_{D1} values (Fig. 5A) and in 1 mM Ca^{2+} using K_{D1} values (Fig. 5B) by subtracting the $\Delta\Delta G$ that results from replacing Phe-1013 with glycine in a wild-type background from the $\Delta\Delta G$ that results from the same substitution made in a Y1021K background. These analyses demonstrate that the degree of coupling between Phe-1013 and Tyr-1021 in DHP binding is highly dependent on the occupancy of the

TABLE 1

Effects glutamate substitutions in the Ca^{2+} channel pore have on Ca^{2+} and DHP binding parameters

Values are means \pm S.E.M.

	K_{D1}	αK_{D1}	K_{C1}	αK_{C1}	α
	nM (-fold change)		μM (-fold change)		-fold change
Wild type	0.31 \pm 0.031	4.8 \pm 0.59	0.040 \pm 0.005	0.62 \pm 0.10	15.5 \pm 1.90
E292Q	0.93 \pm 0.15 (3)*	50.7 \pm 10 (10.6)*	0.462 \pm 0.08 (11.6)*	23.0 \pm 1.5 (37)*	54.5 \pm 11.3 (3.5)*
E614Q	2.68 \pm 1.4 (8.6)*	13.5 \pm 3.1 (2.8)*	5.83 \pm 0.83 (146)*	29.2 \pm 6.6 (47)*	5.11 \pm 1.32 (0.3)
E1014Q	1.71 \pm 0.29 (5.5)*	7.71 \pm 0.80 (1.6)	3.72 \pm 1.74 (93)*	20.6 \pm 4.1 (33)*	4.45 \pm 0.48 (0.3)*
E1323Q	2.88 \pm 0.50 (9.3)*	28.1 \pm 3.7 (5.8)*	4.05 \pm 0.10 (101)*	35.6 \pm 2.3 (57)*	9.75 \pm 1.3 (0.6)
E292K	2.69 \pm 0.73 (8.7)*	17.3 \pm 4.0 (3.6)*	6.17 \pm 1.9 (154)*	34.4 \pm 2.6 (55)*	6.40 \pm 1.5 (0.4)
E614K	N.D.	N.D.	N.D.	N.D.	N.D.
E1014K	2.98 \pm 0.68 (9.6)*	3.98 \pm 0.25 (0.8)	4.20 \pm 2.6 (105)*	5.42 \pm 3.1 (8.7)*	1.33 \pm 0.09 (0.1)*
E1323K	N.D.	N.D.	N.D.	N.D.	N.D.

N.D., not determined.

* Values that are significantly different from wild type, as determined by the Student's independent *t* test ($P < 0.05$). Each value is determined from 3 to 14 experiments (see *Materials and Methods* for details).

TABLE 2

Effects nonglutamate substitutions in the Ca^{2+} channel pore have on Ca^{2+} and DHP binding parameters

Values are means \pm S.E.M.

	K_{D1}	αK_{D1}	K_{C1}	αK_{C1}	α
	nM (-fold change)		μM (-fold change)		-fold change
Wild type	0.31 \pm 0.031	4.8 \pm 0.59	0.040 \pm 0.005	0.62 \pm 0.10	15.5 \pm 1.90
C288A	0.25 \pm 0.02 (0.8)	3.63 \pm 0.03 (0.8)	0.075 \pm 0.01 (1.8)	1.09 \pm 0.22 (1.8)	14.5 \pm 1.0 (0.9)
F1013G	0.22 \pm 0.01 (0.7)	42.6 \pm 10.0 (8.9)*	0.017 \pm 0.008 (0.4)	3.37 \pm 1.48 (5.4)*	194 \pm 48 (12.5)*
Q1018M	0.31 \pm 0.03 (0.0)	2.74 \pm 0.12 (0.6)	0.041 \pm 0.004 (0.0)	0.36 \pm 0.04 (0.6)	8.88 \pm 0.38 (0.6)
Q1018E	0.25 \pm 0.02 (0.8)	5.56 \pm 1.7 (1.2)	0.028 \pm 0.005 (0.7)	0.61 \pm 0.21 (0.0)	22.0 \pm 6.7 (1.4)
Y1021K	0.94 \pm 0.05 (3.0)*	7.05 \pm 0.45 (1.5)	1.25 \pm 0.69 (31.3)*	9.38 \pm 5.7 (15.1)*	7.51 \pm 0.48 (0.5)
C1319A	0.30 \pm 0.03 (0.0)	2.85 \pm 0.08 (0.6)	0.048 \pm 0.05 (1.2)	0.45 \pm 0.03 (0.7)	9.5 \pm 0.27 (0.6)
Q1326H	0.57 \pm 0.16 (1.8)	7.40 \pm 0.71 (1.5)	0.046 \pm 0.005 (1.1)	0.60 \pm 0.12 (0.0)	13.1 \pm 1.2 (0.8)
E1327N	0.59 \pm 0.17 (1.9)	4.77 \pm 0.13 (0.0)	0.065 \pm 0.02 (1.6)	0.53 \pm 0.17 (0.8)	8.08 \pm 0.22 (0.5)
FY/GK	7.51 \pm 0.92 (24.3)*	93.9 \pm 14.2 (20.6)*	0.237 \pm 0.08 (5.9)*	3.00 \pm 1.2 (4.8)*	12.5 \pm 1.9 (0.8)

* Values that are significantly different from wild type, as determined by the Student's independent *t* test ($P < 0.05$). Each value is determined from 3 to 14 experiments (see *Materials and Methods* for details).

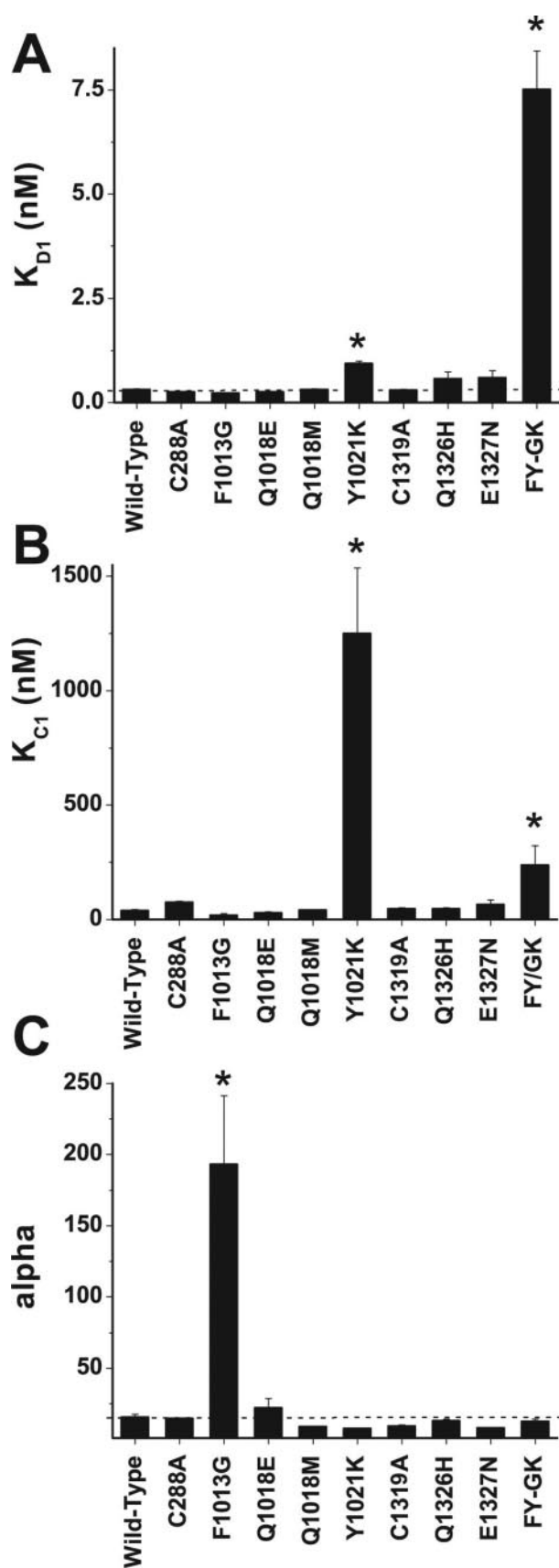


Fig. 4. Nonglutamate residues in the pore segment of domain III are critical for DHP and Ca^{2+} binding. A to C, nonglutamate residues in the pores of repeats I, III, and IV were altered and analyzed as described in Fig. 3.

selectivity filter by Ca^{2+} . The coupling energy in nominally zero Ca^{2+} of 0.08 kcal/mol is negligible (Fig. 5A). This near-zero coupling energy indicates that, in the absence of Ca^{2+} (i.e., state $[\alpha_1]$ of Fig. 2B, Scheme 1), Phe-1013 and Tyr-1021 are not energetically coupled. In contrast, the coupling energy between Phe1013 and Tyr-1021 determined in 1 mM Ca^{2+} is substantial. Replacing Phe-1013 with glycine is highly dependent on whether the substitution is placed in a wild-type backbone (+0.22 kcal/mol) versus the Y1021K backbone (−1.23 kcal/mol). Therefore, when the selectivity filter is occupied by a single Ca^{2+} ion (i.e., state $[\text{Ca}/\alpha_1]$ of Fig. 2B, Scheme 1), Phe-1013 and Tyr-1021 are strongly coupled with an energy of 1.45 kcal/mol [(+0.22 kcal/mol) − (−1.23 kcal/mol) = 1.45 kcal/mol]. This “coupled state”, in which Phe-1013 and Tyr-1021 are energetically coupled and a single Ca^{2+} ion is bound, may represent a stably blocked, nonconducting state of the channel, as is addressed in the discussion below.

The Coupling Factor α Plays an Important Role in Determining the Ca^{2+} Dependence of DHP Binding. The effects of the coupling factor α on the Ca^{2+} dependence of DHP binding to the mutant Ca^{2+} channels are illustrated in Fig. 6. These relationships between DHP binding affinity (K_{D1}^{-1} and αK_{D1}^{-1} in nanomolar $^{-1}$) and Ca^{2+} concentration were simulated from the binding model in Fig. 2B, Scheme 1 and the binding parameters from Table 1. The DHP affinity of E292Q is 11-fold less than that of wild type with no Ca^{2+} ions bound to selectivity filter, but because of a 3.5-fold increase in α compared with wild type, the affinity is decreased by only 3-fold when one Ca^{2+} ion is bound (Fig. 6A). In contrast to E292Q, α values for the other glutamate mutants are smaller than those of wild type (Fig. 3). Consequently, the increases in DHP affinity upon binding of a

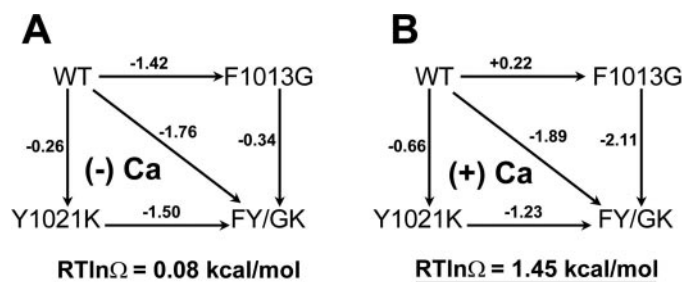


Fig. 5. Ca^{2+} binding to the selectivity filter promotes energetic coupling between Phe-1013 and Tyr-1021. Double mutant cycle analysis was used to measure the coupling energy between Phe-1013 and Tyr-1021 in the absence (A) and presence (B) of a single Ca^{2+} ion in the selectivity filter. PN200-110 binding to its receptor site is driven by a negative change in Gibbs free energy, ΔG . ΔG changes for mutant channels whose affinity for DHP binding is altered and this change in ΔG , designated $\Delta\Delta G$, is calculated using the dissociation constants for drug binding to the wild-type and mutant channels, such that $\Delta\Delta G = -RT\ln(K_{Dmut}/K_{Dwt})$, where R is the gas constant and T is the absolute temperature in Kelvin. $\Delta\Delta G$ values (kilocalories per mole) for each mutant channel are noted by numbers adjacent to arrows. Thermodynamic mutant cycle analysis is based on the principle that the $\Delta\Delta G$ value resulting from the simultaneous alteration of two amino acids is equal to the sum of the $\Delta\Delta G$ values for the individual substitutions that lead to the double mutant. For example, note in A that the $\Delta\Delta G$ for the double mutant FY/GK (−1.76 kcal/mol) is equal to the sum of the $\Delta\Delta G$ values for the individual steps that lead to FY/GK [i.e., (−1.42) + (−0.34)] and [(−0.26) + (−1.50)]. The coupling energy ($RT\ln\Omega$) between two amino acids can be determined by calculating the difference between the $\Delta\Delta G$ values associated with the horizontal (or vertical) arrows as described in the text. Notice that Phe-1013 and Tyr-1021 are strongly coupled only when a single Ca^{2+} ion is bound to the selectivity filter (also see Fig. 2B, vertical box).

single Ca^{2+} ion to these mutants are much less than for E292Q or wild type, as illustrated for E292K in Fig. 6A. In the absence of Ca^{2+} , the DHP binding affinity for mutants E1014K and E1014Q are nearly identical to that of wild type (Fig. 6B). Increasing Ca^{2+} concentration has even less effect on DHP binding for E1014Q and E1014K (Fig. 6B) than for E292Q (Fig. 6A).

The largest change in the magnitude of α was observed with mutant F1013G, whose value for α is 12.5-fold greater than that of wild type (Table 2). Although the affinity of mutant F1013G for DHPs is more than 11-fold lower than wild type in the absence of Ca^{2+} , there is little difference in DHP binding affinity between wild type and F1013G when one Ca^{2+} ion is bound (Fig. 6C). In contrast, the affinity for DHP binding of Y1021K is similar to wild type in the absence of Ca^{2+} but 3-fold less than wild type when one Ca^{2+} ion is bound. This difference in the effect of Ca^{2+} on DHP binding to F1013G and Y1021K results from the 12.5-fold increase in α observed for F1013G compared with the 2-fold decrease in α for Y1021K. Overall, these comparisons illustrate that the coupling factor α is a key determinant of the effect of Ca^{2+} on DHP binding and of DHP affinity under physiological conditions.

Discussion

Ca^{2+} binding to the pore of the L-type Ca^{2+} channels is allosterically coupled to DHP binding, which suggests that the binding of DHPs and Ca^{2+} promotes reciprocal structural rearrangements in the outer pore that alter the functional behavior of the channel. To better understand the roles amino acid residues residing in the outer pore have on DHP binding, permeation and gating, the binding properties of 16 mutant Ca^{2+} channels were assessed using Fig. 2B, Scheme 1. In addition to dramatic changes in the dissociation constants for DHP and Ca^{2+} binding, we found that the coupling factor α plays a major role in determining the pharmacological properties of the mutant channels. For example, α for the nonglutamate mutant F1013G is increased nearly 200-fold, whereas α for Y1021K is only one-half that of wild type. Thermodynamic mutant cycle analysis of these mutants indicates that Phe-1013 and Tyr-1021 are energetically coupled only when the outer pore is occupied by a single Ca^{2+} ion. Our findings are discussed in the context of current theoretical models for permeation (Nonner et al., 1998; Boda et al., 2001; Lipkind and Fozzard, 2001; Wang et al., 2005). We propose that DHPs block monovalent and divalent currents by stabilizing a nonconducting blocked state that is structurally and functionally analogous to a channel with a single Ca^{2+} ion in its selectivity filter.

Binding of DHP Antagonists and Ca^{2+} Stabilize a Blocked Conformation of the Outer Pore. In the absence of Ca^{2+} , the outer pore is held in an *open* conformation ($[\alpha_1]$) by electrostatic repulsion between the four glutamate residues of the EEEE locus. When a single Ca^{2+} ion enters the selectivity filter, it acts as a countercharge and draws the four glutamate residues together to form a *blocked* conformation ($[\text{Ca}/\alpha_1]$) (Lipkind and Fozzard, 2001). According to Fig. 2B, Scheme 1, DHP binding interacts allosterically with Ca^{2+} to stabilize the blocked conformation, thereby preventing Ca^{2+} conductance. Neutralizing any one of the four glutamate residues would destabilize this blocked conformation

by reducing the magnitude of the attractive forces between the bound Ca^{2+} ion and the partially neutralized selectivity filter. In Fig. 3, the K_{D1} values for the glutamate-to-glutamine mutants are all larger than that of wild type. We postulate that neutralization of the residues in the selectivity filter would destabilize the open conformation of the outer pore as well, because the magnitude of the repulsive forces between the four glutamate residues would be decreased. The simulations in Fig. 6 show reduced DHP binding in the absence of Ca^{2+} , indicating that this postulate holds true.

Introduction of Positively Charged Lysine Residues Mimics Binding of Ca^{2+} . Replacing the substituted glutamine residues with positively charged lysine residues would be expected to partially mimic a Ca^{2+} ion by acting as a countercharge in the selectivity filter. If the charge-reversal substitutions were to perfectly mimic a single bound Ca^{2+} ion in the pore, αK_{D1} would equal K_{D1} , and the coupling factor α would equal 1. We were pleased to find that the charge-reversal substitutions did follow this predicted trend, but as might be expected, inserting a lysine with a valence of only +1 into a constrained position in the selectivity filter does not perfectly mimic a free divalent Ca^{2+} ion in the pore. The affinity for DHP binding in nominal Ca^{2+} (i.e., $1/\alpha K_{D1}$) to E292K and E1014K membranes is 3- and 2-fold higher than their charge-neutralized counterparts (Fig. 6). These findings indicate that the introduction of a positive charge in the selectivity filter makes the $[\alpha_1]$ state of the outer pore behave more like the Ca^{2+} -bound $[\text{Ca}/\alpha_1]$ state.

The charge-reversal mutants are still sensitive to Ca^{2+} , but the -fold change in binding affinity that occurs as the channel transitions from $[\alpha_1]$ to $[\text{Ca}/\alpha_1]$ (i.e., the coupling factor α) is reduced. This reduction occurs because replacing the neutral glutamine residues with positively charged lysine residues introduces repulsive forces between the positively charged amine of the lysine residue and the incoming Ca^{2+} ion. Consequently, α values for E292K and E1014K are decreased 8.5- and 3.3-fold compared with their glutamine-substituted counterparts. The combined effects on αK_{D1} and α indicate that the introduction of a positive charge in the pore partially mimics a single Ca^{2+} ion coordinated in the selectivity filter.

Mechanism for DHP Action. The cooperativity between DHP and Ca^{2+} binding suggests that DHPs modulate channel gating by promoting conformational changes in the outer pore. We used a "volume exclusion/charge neutralization" model to explain the reduced conductance of Ba^{2+} but not Ca^{2+} through the pores of $\text{Ca}_v1.2$ correlates of F1013G, Y1021K, and FY/GK (Wang et al., 2005). The crystal diameters of Ca^{2+} and Na^+ ions are nearly identical (2.00 versus 2.04 Å, respectively), yet each Ca^{2+} ion carries twice as much countercharge as a Na^+ ion. Therefore, Ca^{2+} binds tightly to the selectivity filter because it is able to neutralize the highly charged EEEE locus without overcrowding it with counterions. Ba^{2+} and Ca^{2+} ions carry the same charge, but the ionic diameter of Ba^{2+} is approximately 36% larger than that of Ca^{2+} . Thus, Ba^{2+} ions exhibit a higher degree of crowding, lower binding affinity and consequential faster exit rate (i.e., larger conductance) than Ca^{2+} ions. These results suggest that Ba^{2+} conductance is reduced because Ba^{2+} ions in mutant pores are less prone to overcrowding (Wang et al., 2000).

According to Fig. 2B, Scheme 1, Ca^{2+} and DHP binding shifts the configuration of the outer pore from an open state

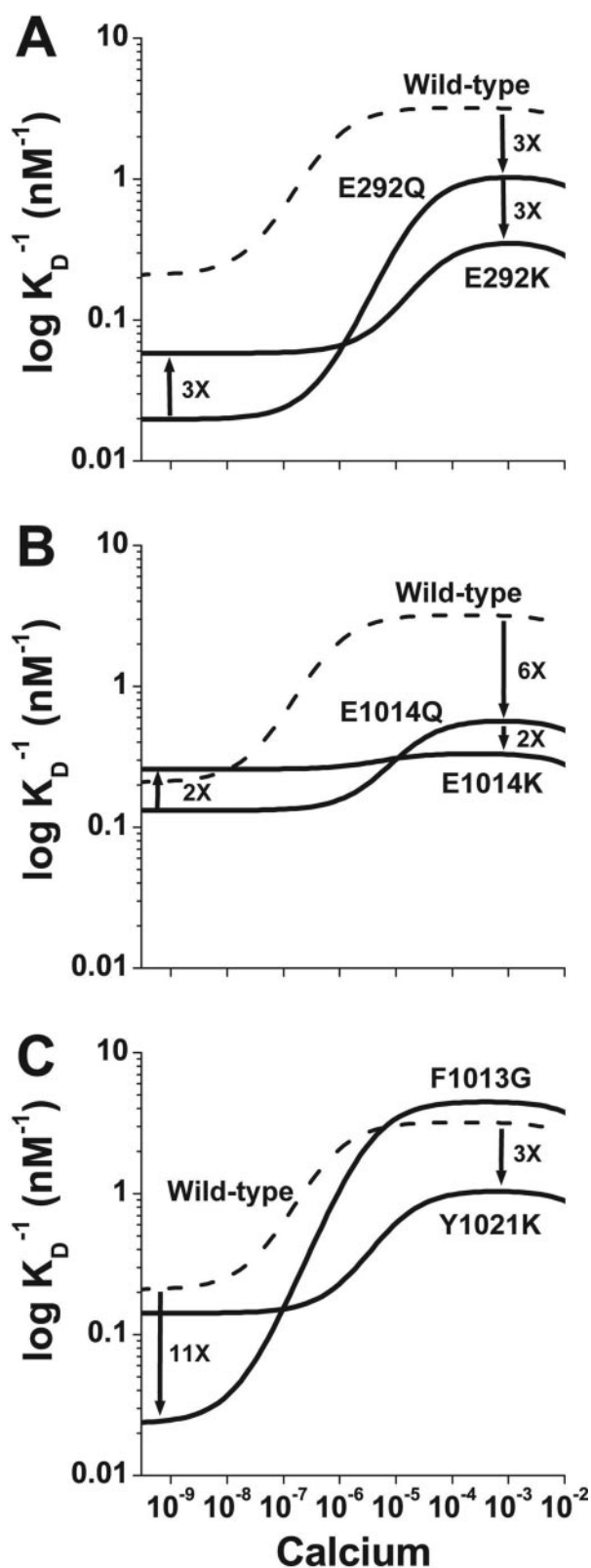


Fig. 6. Substitution of positively charged lysine residues in the selectivity filter partially mimics a bound Ca^{2+} ion. Simulations of $[^3\text{H}]\text{PN200-110}$ binding affinity (nanomolar $^{-1}$) versus free Ca^{2+} for wild type (dashed lines) and the mutants E292Q and E292K (A), E1014Q and E1014K (B), and F1013G and Y1021K (C) are plotted using the binding parameters from Tables 1 and 2. The expression levels of E614K and E1323K were too low to use in these analyses. The -fold differences between the DHP binding affinities of wild-type and/or mutant channels are indicated by numbers adjacent to arrows.

to a blocked state. $[\alpha_1]$ or $[2\text{Ca}/\alpha_1]$ are designated as conducting states in Fig. 2B, Scheme 1, because they represent channels conducting monovalent and divalent currents, respectively. The blocked state, $[\text{Ca}/\alpha_1]$, is designated as a nonconducting state because single Ca^{2+} ions are known to block both monovalent and divalent (i.e., Ba^{2+}) currents (Almers et al., 1984; Hess and Tsien, 1984; Hille, 2001). Here, we combine the volume exclusion/charge neutralization model with Fig. 2B, Scheme 1, and propose that DHPs block mono- and divalent currents through the open $[\alpha_1]$ and $[2\text{Ca}/\alpha_1]$ states of the outer pore by stabilizing a nonconducting blocked state that is structurally and functionally analogous to $[\text{Ca}/\alpha_1]$.

This postulate is consistent with the structural model of Lipkind and Fozzard (2001). In this model, the eight carboxyl groups from the EEEE locus are thought to form three binding sites: a central high-affinity divalent cation binding site formed by four carboxyl groups flanked by two low-affinity sites, each composed of two carboxyl groups (Lipkind and Fozzard, 2001). Divalent cation permeation through such a pore would depend on the occupancy of the two low-affinity sites, thus producing a conducting state ($[2\text{Ca}/\alpha_1]$). Ion permeation would be prevented if the central, high-affinity site were occupied by a single Ca^{2+} ion, thus producing a nonconducting state ($[\text{Ca}/\alpha_1]$). In the absence of divalent cations, repulsive forces in the EEEE locus would open the pore to greater than 4 Å and allow the passage of monovalent cations through the pore, thus producing a conducting state for monovalent cations ($[\alpha_1]$).

Given this scenario, the outer pore of an activated channel would switch between conducting ($[2\text{Ca}/\alpha_1]$) and nonconducting, blocked ($[\text{Ca}/\alpha_1]$) states. The overall open probability of a channel would be determined by the probability that the inner gate is open and the probability that the channel is not in state $[\text{Ca}/\alpha_1]$, which is dependent on the dwell time of the single blocking Ca^{2+} ion residing in the selectivity filter. We propose that DHP antagonists increase this dwell time and that the open probability of the channel decreases as a consequence. It will require single-channel measurements to determine whether the mean open times decrease in the presence of DHP antagonists. Such experiments are very challenging using $\text{Ca}_v1.1$ channels, so this hypothesis will be tested using the cardiac $\text{Ca}_v1.2$ channel.

Energetic Coupling Mediated by Bound Ca^{2+} . The conformational changes that underlie the transitions between the open and blocked states of the outer pore and modulate DHP binding affinity are dependent on the magnitude of the coupling factor α . We used thermodynamic mutant cycle analysis to assess the transition of the outer pore between the open and blocked states, $[\alpha_1]$ and $[\text{Ca}/\alpha_1]$, respectively. Our results demonstrate that Phe-1013 and Tyr-1021 are strongly coupled only when the selectivity filter is occupied by a single Ca^{2+} ion and not when the selectivity filter is unoccupied by Ca^{2+} (Fig. 2B, Scheme 1, box). It seems that the bound Ca^{2+} ion serves to mediate energetic coupling between these two aromatic amino acid residues, which are located on either side of Glu-1014 (Fig. 1). This coupling may result from electronic interactions between the two aromatic residues through the bound Ca^{2+} ion, structural rearrangements in the selectivity filter caused by Ca^{2+} binding, or both. We postulate that Phe-1013 and Tyr-1021 are energetically coupled when the pore is in a blocked,

nonconducting state, and that DHP antagonists block the channel by stabilizing this same nonconducting conformational state. The positive energetic coupling between Phe-1013 and Tyr-1021 revealed here is likely to make a major contribution to the stability of this Ca^{2+} -bound, blocked state.

Acknowledgments

We thank Gregory M. Lipkind for insightful comments on the manuscript.

References

- Almers W and McCleskey EW (1984) Non-selective conductance in calcium channels of frog muscle: calcium selectivity in a single-file pore. *J Physiol (Lond)* **353**:585–608.
- Almers W, McCleskey EW, and Palade PT (1984) A non-selective cation conductance in frog muscle membrane blocked by micromolar external calcium ions. *J Physiol (Lond)* **353**:565–583.
- Bean BP (1984) Nitrendipine block of cardiac calcium channels: high-affinity binding to the inactivated state. *Proc Natl Acad Sci USA* **81**:6388–6392.
- Boda D, Henderson D, and Busath DD (2001) Monte Carlo simulations of the mechanism for channel selectivity: the competition between volume exclusion and charge neutrality. *J Phys Chem* **104**:11574–11577.
- Brown AM, Kunze DL, and Yatani A (1984) The agonist effect of dihydropyridines on Ca channels. *Nature (Lond)* **311**:570–572.
- Carter PJ, Winter G, Wilkinson AJ, and Fersht AR (1984) The use of double mutants to detect structural changes in the active site of the tyrosyl-tRNA synthetase (*Bacillus stearothermophilus*). *Cell* **38**:835–840.
- Cohen CJ and McCarthy RT (1987) Nimodipine block of calcium channels in rat anterior pituitary cells. *J Physiol (Lond)* **387**:195–225.
- Corry B, Allen TW, Kuyucak S, and Chung SH (2001) Mechanisms of permeation and selectivity in calcium channels. *Biophys J* **80**:195–214.
- Dang TX and McCleskey EW (1998) Ion channel selectivity through stepwise changes in binding affinity. *J Gen Physiol* **111**:185–193.
- Glossmann H, Ferry DR, Goll A, Striessnig J, and Zernig G (1985) Calcium channels and calcium channel drugs: recent biochemical and biophysical findings. *Arzneimittelforschung* **35**:1917–1935.
- Gurney AM, Nerbonne JM, and Lester HA (1985) Photoinduced removal of nifedipine reveals mechanisms of calcium antagonist action on single heart cells. *J Gen Physiol* **86**:353–379.
- Hamilton SL, Yatani A, Brush K, Schwartz A, and Brown AM (1987) A comparison between the binding and electrophysiological effects of dihydropyridines on cardiac membranes. *Mol Pharmacol* **31**:221–231.
- He M, Bodi I, Mikala G, and Schwartz A (1997) Motif III S5 of L-type calcium channels is involved in the dihydropyridine binding site. A combined radioligand binding and electrophysiological study. *J Biol Chem* **272**:2629–2633.
- Hess P, Lansman JB, and Tsien RW (1984) Different modes of Ca channel gating behaviour favoured by dihydropyridine Ca agonists and antagonists. *Nature (Lond)* **311**:538–544.
- Hess P and Tsien RW (1984) Mechanism of ion permeation through calcium channels. *Nature (Lond)* **309**:453–456.
- Hidalgo P and MacKinnon R (1995) Revealing the architecture of a K^+ channel pore through mutant cycles with a peptide inhibitor. *Science (Wash DC)* **268**:307–310.
- Hille B (2001) *Ion Channels of Excitable Membranes*, Sinauer Associates, Inc., Sunderland, MA.
- Hockerman GH, Peterson BZ, Sharp E, Tanada TN, Scheuer T, and Catterall WA (1997) Construction of a high-affinity receptor site for dihydropyridine agonists and antagonists by single amino acid substitutions in a non-L-type Ca^{2+} channel. *Proc Natl Acad Sci USA* **94**:14906–14911.
- Ito H, Klugbauer N, and Hofmann F (1997) Transfer of the high affinity dihydropyridine sensitivity from L-type to non-L-type calcium channel. *Mol Pharmacol* **52**:735–740.
- Kokubun S, Prod'homme B, Becker C, Porzig H, and Reuter H (1986) Studies on Ca channels in intact cardiac cells: voltage-dependent effects and cooperative interactions of dihydropyridine enantiomers. *Mol Pharmacol* **30**:571–584.
- Kokubun S and Reuter H (1984) Dihydropyridine derivatives prolong the open state of Ca channels in cultured cardiac cells. *Proc Natl Acad Sci USA* **81**:4824–4827.
- Lipkind GM and Fozzard HA (2001) Modeling of the outer vestibule and selectivity filter of the L-type Ca^{2+} channel. *Biochemistry* **40**:6786–6794.
- Mitterdorfer J, Sinnegger MJ, Grabner M, Striessnig J, and Glossmann H (1995) Coordination of Ca^{2+} by the pore region glutamates is essential for high-affinity dihydropyridine binding to the cardiac Ca^{2+} channel α_1 subunit. *Biochemistry* **34**:9350–9355.
- Mitterdorfer J, Wang Z, Sinnegger MJ, Hering S, Striessnig J, Grabner M, and Glossmann H (1996) Two amino acid residues in the IIIS5 segment of L-type calcium channels differentially contribute to 1,4-dihydropyridine sensitivity. *J Biol Chem* **271**:30330–30335.
- Nonner W, Chen DP, and Eisenberg B (1998) Anomalous mole fraction effect, electrostatics and binding in ionic channels. *Biophys J* **74**:2327–2334.
- Peterson BZ and Catterall WA (1995) Calcium binding in the pore of L-type calcium channels modulates high affinity dihydropyridine binding. *J Biol Chem* **270**:18201–18204.
- Peterson BZ, Johnson BD, Hockerman GH, Acheson M, Scheuer T, and Catterall WA (1997) Analysis of the dihydropyridine receptor site of L-type calcium channels by alanine-scanning mutagenesis. *J Biol Chem* **272**:18752–18758.
- Peterson BZ, Tanada TN, and Catterall WA (1996) Molecular determinants of high affinity dihydropyridine binding in L-type calcium channels. *J Biol Chem* **271**:5293–5296.
- Sanguinetti MC and Kass RS (1984) Voltage-dependent block of calcium channel current in the calf cardiac Purkinje fiber by dihydropyridine calcium channel antagonists. *Circ Res* **55**:336–348.
- Sanguinetti MC, Krafte DS, and Kass RS (1986) Voltage-dependent modulation of Ca channel current in heart cells by Bay K8644. *J Gen Physiol* **88**:369–392.
- Sather WA and McCleskey EW (2003) Permeation and selectivity in calcium channels. *Annu Rev Physiol* **65**:133–159.
- Schuster A, Lacinova L, Klugbauer N, Ito H, Birnbaumer L, and Hofmann F (1996) The IVS6 segment of the L-type calcium channel is critical for the action of dihydropyridines and phenylalkylamines. *EMBO (Eur Mol Biol Organ) J* **15**:2365–2370.
- Sinnegger MJ, Wang Z, Grabner M, Hering S, Striessnig J, Glossmann H, and Mitterdorfer J (1997) Nine L-type amino acid residues confer full 1,4-dihydropyridine sensitivity to the neuronal calcium channel α_{1A} subunit. Role of L-type Met1188. *J Biol Chem* **272**:27686–27693.
- Thomas G, Chung M, and Cohen CJ (1985) A dihydropyridine (Bay k 8644) that enhances calcium currents in guinea pig and calf myocardial cells. A new type of positive inotropic agent. *Circ Res* **56**:87–96.
- Wang X, Ponoran TA, Rasmusson RL, Ragsdale DS, and Peterson BZ (2005) Amino acid substitutions in the pore of the $\text{CaV}1.2$ calcium channel reduce barium currents without affecting calcium currents. *Biophys J* **89**:1731–1743.
- Yue DT and Marban E (1990) Permeation in the dihydropyridine-sensitive calcium channel. Multi-ion occupancy but no anomalous mole-fraction effect between Ba^{2+} and Ca^{2+} . *J Gen Physiol* **95**:911–939.

Address correspondence to: Dr. Blaise Z. Peterson, Cellular and Molecular Physiology, H166, Penn State Milton S. Hershey Medical Center, College of Medicine, 500 University Dr., Room C6603, P.O. Box 850, Hershey, PA 17033-0850. E-mail: bpeterson@psu.edu